

Spin energetics in a GaAs quantum well: Asymmetric spin-flip Raman scattering

D. Richards

Cavendish Laboratory, Madingley Road, Cambridge CB3 0HE, United Kingdom

B. Jusserand

France Télécom, CNET/DTT, Laboratoire de Bagneux, 196 Avenue Henri Ravera, F-92220 Bagneux, France

(Received 9 July 1998)

We demonstrate an asymmetric dependence of the spin-flip electronic Raman spectrum from a two-dimensional electron gas on the direction of circular polarization of the photons, resulting from an interference of light scattered from longitudinal and transverse spin-density fluctuations. By exploiting these selection rules, we are able to determine experimentally that the sign of the band-structure parameter a_{42} , which describes the bulk k^3 conduction-band spin splitting in zinc-blende semiconductors, is *negative* for GaAs.
[S0163-1829(99)50504-3]

The lack of inversion symmetry in zinc-blende semiconductors, such as GaAs, results in a removal of spin degeneracy for conduction band electrons with wave vectors k away from the Brillouin zone center, even in the absence of a magnetic field.^{1,2} In addition to this bulk inversion asymmetry (BIA) spin splitting, the presence of an electric field results in an additional contribution, referred to as the Rashba spin splitting.³ In recent years there has been considerable interest in the conduction band spin splitting in semiconductor quantum wells, both theoretically⁴⁻⁶ and experimentally, through measurements of electronic Raman scattering,⁷ weak antilocalization^{8,9} and Shubnikov-de Haas oscillations¹⁰ in two-dimensional electron gas (2DEG) systems.

In particular, from Raman scattering measurements of spin-flip single particle excitations (SPE) in a 2DEG we have been able to determine the in-plane anisotropy of the spin splitting and demonstrate the importance of both the BIA and Rashba contributions to the spin-splitting in asymmetrically-doped quantum wells;^{11,12} calculations of the spin-splitting within a multiband envelope function approach have demonstrated good agreement between these experiments and theory.¹³ Using a perturbative approach^{4,12} based on the theoretically well-known bulk spin splitting,¹ we were able to extract the magnitudes of the bulk spin-splitting parameters a_{42} (used to describe the BIA spin-splitting to k^3) and a_{64} (for the Rashba splitting, proportional to k),⁴ which were in good agreement with values predicted within $\mathbf{k}\cdot\mathbf{p}$ theory.^{1,2,4} However, we were unable to determine from these measurements the *absolute sign* of a_{42} or a_{64} , although we were able to demonstrate the opposite sign⁴ of the two parameters.^{11,12}

Mal'shukov *et al.*¹⁴ predicted recently that an interference of light amplitudes scattered from longitudinal and transverse spin-density fluctuations leads to an asymmetric dependence of the Raman spectrum on the direction of circular polarization of the photons. We exploit these selection rules here to determine experimentally the sign of a_{42} (defined as positive if the energy of a spin-up electron with wavevector $\mathbf{k}||[110]$ in bulk GaAs is greater than that of a spin-down electron). Theoretical determinations of the sign of a_{42} for

GaAs appear to disagree; the sign is given as negative in Ref. 4 whereas the spin-splitting parameter γ_c ($\equiv 2a_{42}$) determined in Ref. 2 is positive.

If we adopt a perturbative approach to describe the spin-splitting in a quantum well, the energies of the conduction band states for a wave vector \mathbf{k} are given by $E_{\uparrow}(\mathbf{k}) = E_0(\mathbf{k}) + |\mathbf{h}(\mathbf{k})|$ and $E_{\downarrow}(\mathbf{k}) = E_0(\mathbf{k}) - |\mathbf{h}(\mathbf{k})|$, where E_0 is the energy in the absence of spin splitting and $\mathbf{h}(\mathbf{k})$ acts as an effective magnetic field,¹⁴ given by^{1,11}

$$\begin{aligned} h_x &= a_{42}k_x(k_y^2 - \kappa^2) - a_{64}\epsilon_z k_y, \\ h_y &= a_{42}k_y(\kappa^2 - k_x^2) + a_{64}\epsilon_z k_x, \\ h_z &= 0, \end{aligned} \quad (1)$$

where κ is a confinement wave vector along the z axis⁷ and ϵ_z is an effective electric field^{11,12} for electrons in the quantum well; the x , y , and z axes are parallel to the $\langle 100 \rangle$ directions of the semiconductor. The unit vector $\mathbf{n}_{\mathbf{k}} = \mathbf{h}(\mathbf{k})/|\mathbf{h}(\mathbf{k})|$ describes the orientation of \mathbf{h} .

For SPE of energy ω and wave vector \mathbf{q} , the cross-section $R(\mathbf{q}, \omega)[\mathbf{e}_i, \mathbf{e}_s]$ (\mathbf{e}_i and \mathbf{e}_s are the polarizations of the incident and scattered photons) for Raman scattering by spin-density fluctuations is given by:^{14,15}

$$R(\mathbf{q}, \omega)[\mathbf{e}_i, \mathbf{e}_s] \propto -(N(\omega) + 1) \sum_{i,j=\uparrow,\downarrow} \text{Im}[\Pi_{ij}(\mathbf{q}, \omega)], \quad (2)$$

$$\Pi_{ij}(\mathbf{q}, \omega) = \sum_{\mathbf{k}} M_{\mathbf{k},i,j} \frac{f[E_i(\mathbf{k}+\mathbf{q})] - f[E_j(\mathbf{k})]}{E_i(\mathbf{k}+\mathbf{q}) - E_j(\mathbf{k}) - \omega - i\delta}. \quad (3)$$

$N(\omega)$ and $f(E)$ are the Bose-Einstein and Fermi-Dirac occupation factors. $M_{\mathbf{k},i,j}(\mathbf{q}, \omega)$ describes the transition probability for SPE from state \mathbf{k} in spin-subband j [energy $E_j(\mathbf{k})$] to state $\mathbf{k}+\mathbf{q}$ in spin-subband i [energy $E_i(\mathbf{k}+\mathbf{q})$].¹⁴ If $M_{\mathbf{k},i,j}$ is independent of \mathbf{k} , then Eq. (3) reduces to $\Pi_{ij} = M_{ij} \chi_{ij}^0$, where χ_{ij}^0 is the Lindhard polarizability for transitions between spin-subbands j and i .¹⁵

For spin-flip SPE, Mal'shukov *et al.* have shown that¹⁴

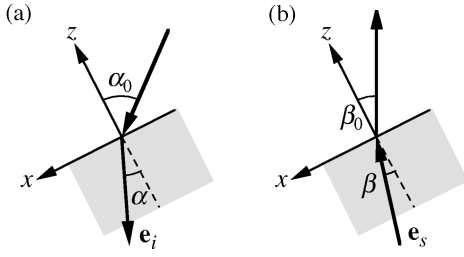


FIG. 1. Light scattering geometry for (a) incident light and (b) scattered light. The x -axis is parallel to the $[100]$ direction of the sample; z is parallel to $[001]$.

$$\begin{pmatrix} M_{\mathbf{k},\uparrow,\downarrow} \\ M_{\mathbf{k},\downarrow,\uparrow} \end{pmatrix} = \gamma^2 \left(|\mathbf{P}_{\parallel} \times \mathbf{n}_{\mathbf{k}}|^2 + |P_z|^2 \begin{pmatrix} + \\ - \end{pmatrix} i\mathbf{P} \times \mathbf{P}^* \cdot \mathbf{n}_{\mathbf{k}} \right), \quad (4)$$

where γ is a constant¹⁵ and $\mathbf{P} = \mathbf{e}_i \times \mathbf{e}_s^*$ (\mathbf{e}_i and \mathbf{e}_s are defined with respect to the sample). It was pointed out in Ref. 14 that if the polarizations of the incident and scattered light are circular then reversal of the polarizations, such that $\mathbf{e}_i \rightarrow \mathbf{e}_i^*$ and $\mathbf{e}_s \rightarrow \mathbf{e}_s^*$, results in $\mathbf{P} \rightarrow \mathbf{P}^*$, leading to a change of sign of the last term of Eq. (4). Thus the resulting Raman difference spectrum $\Delta R(\mathbf{q}, \omega) = R[\mathbf{e}_i, \mathbf{e}_s] - R[\mathbf{e}_i^*, \mathbf{e}_s^*]$, obtained by reversing the circular polarizations of both incident and scattered light, should contain only contributions resulting from this term. Non-spin-flip SPE and the contribution to spin-flip SPE from the first two terms in Eq. (4) will be unaffected by the polarization reversal and will therefore not contribute to the difference spectrum.¹⁴

The light scattering geometry for the Raman measurements is shown in Fig. 1. The sample is an asymmetrically modulation-doped 180-Å GaAs/Al_{0.33}Ga_{0.67}As quantum well with a 2DEG density of $1.3 \times 10^{12} \text{ cm}^{-2}$ (described elsewhere;¹¹ sample D in Ref. 12), held at ~ 10 K. The backscattering geometry results in an in-plane wave vector transfer

$$q = \frac{2\pi}{\lambda} [\sin \alpha_0 + \sin \beta_0]$$

to excitations in the 2DEG along the $[100]$ direction. Measurements were performed with an excitation wavelength $\lambda = 776$ nm for two different geometries, parameters for which are given in Table I.

TABLE I. Parameters, described in the text and in Fig. 1, for the two light scattering geometries employed. For the excitation wavelength $\lambda = 776$ nm, the refractive index of the semiconductor is taken to be 3.7.

	A	B
α_0 ($^\circ$)	49.5	30.5
β_0 ($^\circ$)	38.5	19.5
q (10^5 cm^{-1})	1.12	0.68
δ ($^\circ$)	1.5	2.9
ψ ($^\circ$)	11.2	6.8
$2i(\mathbf{P} \times \mathbf{P}^*)_x[\sigma_+, \sigma_+]$	-0.3×10^{-3}	-0.6×10^{-3}
$2i(\mathbf{P} \times \mathbf{P}^*)_x[\sigma_+, \sigma_-]$	-0.10	-0.20

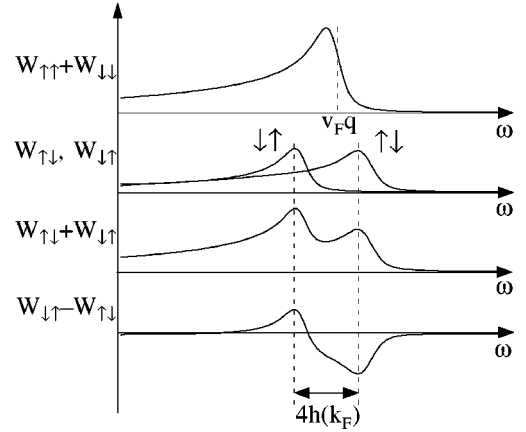


FIG. 2. Theoretical SPE Raman spectra; $W_{ij}(\mathbf{q}, \omega) = -(N+1)\text{Im}[\chi_{ij}^0(\mathbf{q}, \omega)]$. Non-spin-flip spectrum ($W_{\uparrow\uparrow} + W_{\downarrow\downarrow}$) and spin-flip spectra: $W_{\uparrow\downarrow}$, $W_{\downarrow\uparrow}$, ($W_{\uparrow\downarrow} + W_{\downarrow\uparrow}$) (sum spectrum) and $\Delta R \propto (W_{\downarrow\uparrow} - W_{\uparrow\downarrow})$ (difference spectrum). High-energy cut-offs for spin-flip SPE occur at $v_F q \pm 2|\mathbf{h}(k_F)|$.

Within the sample reference frame defined in Fig. 1, the polarization vectors associated with σ_+ (right circularly polarized) incident and scattered light are given by

$$\begin{aligned} \mathbf{e}_i[\sigma_+] &= \frac{1}{\sqrt{2}}(\cos \alpha, i, \sin \alpha), \\ \mathbf{e}_s[\sigma_+] &= \frac{1}{\sqrt{2}}(\cos \beta, -i, \sin \beta). \end{aligned} \quad (5)$$

The corresponding σ_- polarizations are obtained by taking the complex conjugates. Hence, we find for σ_+ polarized incident light and σ_+ polarized scattered light [$z(\sigma_+, \sigma_+)\bar{z}$ scattering],

$$(\mathbf{P} \times \mathbf{P}^*)[\sigma_+, \sigma_+] = 2i \sin \delta \sin \frac{\delta}{2} (\sin \psi, 0, -\cos \psi), \quad (6)$$

where $\delta = \alpha - \beta$, and $\psi = (\alpha + \beta)/2$ (see Table I). For $z(\sigma_+, \sigma_-)\bar{z}$ scattering (σ_+ incident and σ_- scattered),

$$(\mathbf{P} \times \mathbf{P}^*)[\sigma_+, \sigma_-] = 2i \sin \delta \cos \frac{\delta}{2} (\cos \psi, 0, \sin \psi). \quad (7)$$

Note that if $\alpha = \beta$ then $\mathbf{P} \times \mathbf{P}^* = 0$ for all polarizations; therefore there should be no signal in the difference spectrum $\Delta R(\mathbf{q}, \omega)$ for a true backscattering geometry.

From Eqs. (1), (6), and (7) we can see that for the present scattering geometry the only contribution to the interference term in Eq. (4) is $(\mathbf{P} \times \mathbf{P}^*)_x n_x$; values for $2i(\mathbf{P} \times \mathbf{P}^*)_x$ are given for $z(\sigma_+, \sigma_+)\bar{z}$ and $z(\sigma_+, \sigma_-)\bar{z}$ in Table I. Note that $(\mathbf{P} \times \mathbf{P}^*)_x$ is significantly smaller for $z(\sigma_+, \sigma_+)\bar{z}$ than for $z(\sigma_+, \sigma_-)\bar{z}$, suggesting that we should only expect to see a signal in the difference spectrum obtained by changing polarizations from $z(\sigma_+, \sigma_-)\bar{z}$ to $z(\sigma_-, \sigma_+)\bar{z}$.

We are concerned here with Raman scattering by SPE of energy ω and wave vector $q \ll k_F$ (the Fermi wave vector), with \mathbf{q} parallel to $[100]$ (x). We can obtain some insight into the form of the difference spectrum if we make the assump-

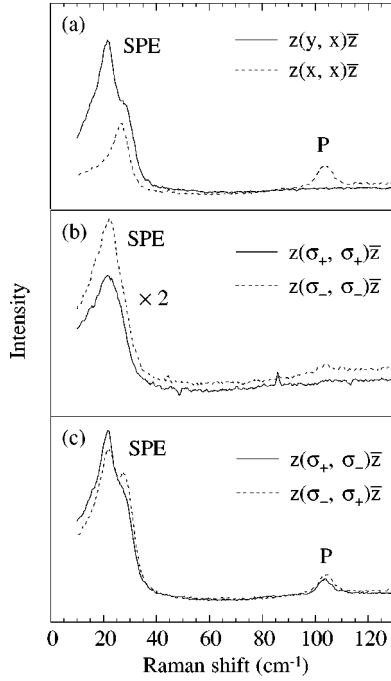


FIG. 3. Raman spectra measured with $q = 1.12 \times 10^5 \text{ cm}^{-1}$ for (a) $z(y,x)\bar{z}$ (line) and $z(x,x)\bar{z}$ (dashes) [cf. Fig. 2], (b) $z(\sigma_+, \sigma_+)\bar{z}$ (line) and $z(\sigma_-, \sigma_-)\bar{z}$ (dashes), (c) $z(\sigma_+, \sigma_-)\bar{z}$ (lines) and $z(\sigma_-, \sigma_+)\bar{z}$ (dashes) polarization configurations. Peaks due to Raman scattering by single particle excitations (SPE) and the plasmon (P) are present.

tion $h(k) \ll v_F q$ (v_F is the Fermi velocity), in which case excitations involving states around $\mathbf{k} = (k_F, 0, 0)$ will dominate the spin-flip SPE Raman spectrum.¹¹ For these states $h_x = -a_{42}k_F\kappa^2$, $h_y = a_{64}\epsilon k_F$, and $h_z = 0$ [see Eq. (1)]. In this case $\mathbf{n}_{\mathbf{k}}$, and hence $M_{\mathbf{k},i,j}$ [see Eq.(4)], is independent of \mathbf{k} and so the change in the Raman scattering cross section on reversal of polarization from $z(\mathbf{e}_i, \mathbf{e}_s)\bar{z}$ to $z(\mathbf{e}_i^*, \mathbf{e}_s^*)\bar{z}$ can be written as

$$\Delta R(\mathbf{q}, \omega) \propto 2i\gamma^2 (\mathbf{P} \times \mathbf{P}^*)_x \frac{a_{42}}{\sqrt{a_{42}^2 + a_{64}^2 \epsilon^2 / \kappa^4}} \times [N(\omega) + 1] \text{Im}[\chi_{\uparrow\downarrow}^0(q, \omega) - \chi_{\downarrow\uparrow}^0(q, \omega)]. \quad (8)$$

We can see from Eq. (8) that the sign of the Raman difference signal $\Delta R(\mathbf{q}, \omega)$ will depend on the sign of a_{42} . If a_{42} is negative⁴ then, using the values for $(\mathbf{P} \times \mathbf{P}^*)_x$ given in Table I, spin-down to spin-up SPE ($R \propto -\text{Im}[\chi_{\uparrow\downarrow}^0]$) lead to a negative signal in the difference spectrum with a minimum at $\omega_{\uparrow\downarrow} = v_F q + 2|\mathbf{h}(k_F)|$, whereas spin-up to spin-down transitions ($R \propto -\text{Im}[\chi_{\downarrow\uparrow}^0]$) give a positive signal in $\Delta R(\mathbf{q}, \omega)$ at smaller Raman shifts, with a maximum at $\omega_{\downarrow\uparrow} = v_F q - 2|\mathbf{h}(k_F)|$. This is illustrated in Fig. 2, where $\chi_{\uparrow\downarrow}^0$ and $\chi_{\downarrow\uparrow}^0$ have been evaluated numerically.⁷ For a detailed comparison of experiment with theory the assumption $h(k) \ll v_F q$ implicit in Eq. (8) is actually not sufficient in the present case and we must instead incorporate $M_{\mathbf{k},i,j}$ directly in our nu-

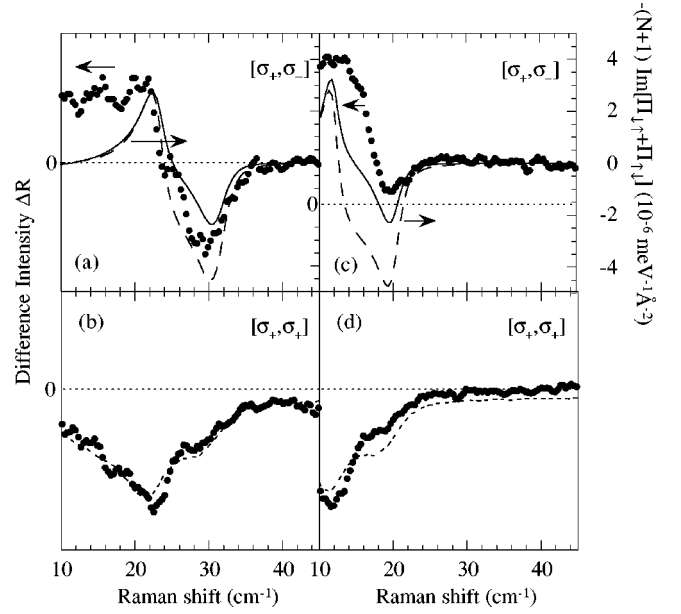


FIG. 4. Experimental Raman difference spectra (●) for $q = 1.12 \times 10^5 \text{ cm}^{-1}$ [(a) and (b)] and $q = 0.68 \times 10^5 \text{ cm}^{-1}$ [(c) and (d)]. (a), (c) ($R[\sigma_+, \sigma_-] - R[\sigma_-, \sigma_+]$). (b), (d) ($R[\sigma_+, \sigma_+] - R[\sigma_-, \sigma_-]$). The dotted lines indicate the zeros for the difference spectra. In (a) and (c) we show calculated spin-flip SPE difference spectra (lines). Spectra obtained using Eq. (8) are also shown (long dashes). In (b) and (d) the spin-flip SPE $z(y,x)\bar{z}$ spectra are superimposed (dashed lines).

merical determination of Π_{ij} [see Eq. (3)], using an expression for n_x in Eq. (4) derived from the full form of $\mathbf{h}(\mathbf{k})$ [Eq. (1)].

In addition to Raman scattering by spin-density fluctuations, described above, we must also consider Raman scattering by charge-density fluctuations, the cross-section for which depends on polarizations as $|\mathbf{e}_i \cdot \mathbf{e}_s^*|^2$.¹⁵ This leads to Raman scattering by plasmons and non-spin-flip SPE if (for small α and β) the polarizations of the incident and scattered light are linear and parallel [e.g., $z(x,x)\bar{z}$], or if the polarizations are circular and of opposite sense [i.e., $z(\sigma_+, \sigma_-)\bar{z}$ or $z(\sigma_-, \sigma_+)\bar{z}$].

We show in Fig. 3 Raman spectra for $q = 1.12 \times 10^5 \text{ cm}^{-1}$ for various polarization configurations. We note that the plasmon (P) at 105 cm^{-1} is only present in the $z(x,x)\bar{z}$, $z(\sigma_+, \sigma_-)\bar{z}$ and $z(\sigma_-, \sigma_+)\bar{z}$ spectra, as expected. The spin-flip and non-spin-flip SPE line shapes are also clearly identifiable in Fig. 3(a) between 0 and 35 cm^{-1} , in the $z(y,x)\bar{z}$ and $z(x,x)\bar{z}$ spectra, respectively. The SPE signal obtained in the $z(\sigma_+, \sigma_+)\bar{z}$ and $z(\sigma_-, \sigma_-)\bar{z}$ spectra [Fig. 3(b)] have the same line shape but slightly different total intensities, possibly due to a change in the total transmission of the experimental setup on reversal of the polarizations. In contrast, for the $z(\sigma_+, \sigma_-)\bar{z}$ and $z(\sigma_-, \sigma_+)\bar{z}$ spectra in Fig. 3(c), the form of the line-shape is changed when the polarizations of the incident and scattered light are reversed.

The polarization states in the sample for nominally circular polarizations will certainly be elliptical in reality due to, e.g., the off-normal incidence at the semiconductor surface.

However, by determining the difference spectra ($R[\sigma_+, \sigma_-] - R[\sigma_-, \sigma_+]$) and ($R[\sigma_+, \sigma_+] - R[\sigma_-, \sigma_-]$), any signals resulting from departures from pure circular polarization should cancel. In addition, photoluminescence signals should be equivalent within each pair of spectra, resulting in no contribution to the difference spectrum, and we should be left only with Raman signals resulting from the interference effects predicted in Ref. 14.

The difference spectra ($R[\sigma_+, \sigma_-] - R[\sigma_-, \sigma_+]$) and ($R[\sigma_+, \sigma_+] - R[\sigma_-, \sigma_-]$) are shown in Fig. 4 for the two wave vectors; no attempt has been made to scale the experimental spectra, which were all obtained under nominally identical conditions. The line shapes of the difference spectra ($R[\sigma_+, \sigma_+] - R[\sigma_-, \sigma_-]$) in Figs. 4(b) and 4(d) are in fact described well by the total spin-flip spectrum obtained with crossed linear polarizations (which are also shown, inverted, in Fig. 4), suggesting an incomplete cancellation of contributions to the Raman spectra other than the interference term of Eq. (4). Indeed, appropriate scaling of $R[\sigma_+, \sigma_+]$ and $R[\sigma_-, \sigma_-]$ can lead to complete cancellation in the corresponding difference spectrum, as predicted by theory.

The ($R[\sigma_+, \sigma_-] - R[\sigma_-, \sigma_+]$) difference spectra in Figs. 4(a) and 4(c) have the same form as that illustrated in Fig. 2 (superimposed on a constant background signal, again probably resulting from slight deviations in the experimental set-up between measurements), giving confirmation of the selection rules predicted by Mal'shukov *et al.* The nonzero

signal at very small Raman shifts in the difference spectra may result from variations between spectra in the intensity of stray light not rejected by the subtractive stage of the triple grating spectrometer. We also show in Figs. 4(a) and 4(c) theoretical spin-flip SPE difference spectra calculated using the full \mathbf{k} -dependent form for $M_{\mathbf{k},i,j}$ in Eq. (3), with $a_{42} = -16.5 \text{ eV \AA}^3$ and $a_{64}\epsilon = -6.9 \text{ meV \AA}$,¹¹ which are in good agreement with the experimental line shapes [difference spectra calculated using Eq. (8) are also shown]. We should note that we were unable to fit ($R[\sigma_+, \sigma_-] - R[\sigma_-, \sigma_+]$) using any combination of the SPE spectra obtained with linear polarizations, as was possible for ($R[\sigma_+, \sigma_+] - R[\sigma_-, \sigma_-]$); the interference effect described in Ref. 14 is essential to account for the overall form of these lineshapes.

In conclusion, we have demonstrated the polarization asymmetry predicted by Mal'shukov *et al.* for spin-flip Raman scattering,¹⁴ obtaining good agreement between experimental and theoretical line shapes. This has enabled us to give an experimental determination of the sign of the band-structure parameter a_{42} in GaAs, which we found to be negative as predicted in Ref. 4.

D.R. is grateful to the Royal Society and the EPSRC for the support of this work. We thank B. Etienne for the provision of the MBE sample used in this work, D. S. Kainth for technical assistance, and U. Rössler for helpful discussions.

- ¹U. Rössler, *Solid State Commun.* **49**, 943 (1984); M. Braun and U. Rössler, *J. Phys. C* **18**, 3365 (1985); H. Mayer and U. Rössler, *Solid State Commun.* **87**, 81 (1993).
²M. Cardona, N. E. Christensen, and G. Fasol, *Phys. Rev. B* **38**, 1806 (1988).
³Yu. A. Bychkov and E. I. Rashba, *J. Phys. C* **17**, 6039 (1984).
⁴F. Malcher, G. Lommer, and U. Rössler, *Superlattices Microstruct.* **2**, 267 (1986).
⁵P. Pfeffer, *Phys. Rev. B* **55**, R7359 (1997); P. Pfeffer and W. Zawadzki, *ibid.* **52**, R14 332 (1995).
⁶E. A. de Andrada e Silva, G. C. La Rocca, and F. Bassani, *Phys. Rev. B* **55**, 16 293 (1997).
⁷B. Jusserand, D. Richards, H. Peric, and B. Etienne, *Phys. Rev. Lett.* **69**, 848 (1992).
⁸P. D. Dresselhaus, C. M. A. Papavassiliou, R. G. Wheeler, and R. N. Sacks, *Phys. Rev. Lett.* **68**, 106 (1992).

- ⁹T. Hassenkam, S. Pedersen, K. Baklanov, K. Kristensen, C. B. Sorensen, P. E. Lindelhof, F. G. Pikus, and G. E. Pikus, *Phys. Rev. B* **55**, 9298 (1997).
¹⁰P. Ramvall, B. Kowalski, and P. Omling, *Phys. Rev. B* **55**, 7160 (1997).
¹¹B. Jusserand, D. Richards, G. Allan, C. Priester, and B. Etienne, *Phys. Rev. B* **51**, 4707 (1995).
¹²D. Richards, B. Jusserand, G. Allan, C. Priester, and B. Etienne, *Solid-State Electron.* **40**, 127 (1996).
¹³L. Wissinger, U. Rössler, R. Winkler, B. Jusserand, and D. Richards, *Phys. Rev. B* **58**, 15 375 (1998).
¹⁴A. G. Mal'shukov, K. A. Chao, and M. Willander, *Phys. Rev. B* **55**, R1918 (1997).
¹⁵G. Abstreiter, M. Cardona, and A. Pinczuk, in *Light Scattering in Solids IV*, edited by M. Cardona and G. Güntherodt (Springer, Heidelberg, 1984), p. 5.